

# A Gaussian Process Model for Ordinal Data with Applications to Chemoinformatics

Arron Gosnell\* and Evangelos Evangelou  
University of Bath, UK

## Abstract

With the proliferation of screening tools for chemical testing, it is now possible to create vast databases of chemicals easily. However, rigorous statistical methodologies employed to analyse these databases are in their infancy, and further development to facilitate chemical discovery is imperative. In this paper, we present conditional Gaussian process models to predict ordinal outcomes from chemical experiments, where the inputs are chemical compounds. We implement the Tanimoto distance, a metric on the chemical space, within the covariance of the Gaussian processes to capture correlated effects in the chemical space. A novel aspect of our model is that the kernel contains a scaling parameter, a feature not previously examined in the literature, that controls the strength of the correlation between elements of the chemical space. Using molecular fingerprints, a numerical representation of a compound’s location within the chemical space, we show that accounting for correlation amongst chemical compounds improves predictive performance over the uncorrelated model, where effects are assumed to be independent. Moreover, we present a genetic algorithm for the facilitation of chemical discovery and identification of important features to the compound’s efficacy. A simulation study is conducted to demonstrate the suitability of the proposed methods. Our proposed methods are demonstrated on a hazard classification problem of organic solvents.

**Keywords:** chemical space; drug discovery; genetic algorithm; molecular fingerprints; quantitative structure-activity relationships; Tanimoto distance

## 1 Introduction

Drug discovery is of vital importance to many fields, including agricultural sciences, chemistry, medicine, and the food and drinks industry. Chemoinformatics, which focuses on the analysis of data from chemical compounds, can aid in the understanding of influential chemical structures and the discovery of novel drugs [2, 26, 32]. Many chemoinformatics methods rely on quantitative structure-activity relationship (QSAR) techniques, which aim to predict biological activities from chemical structures [36, 38, 51]. To that end, chemical graph representations are vital for understanding the relationship between chemical structures and their biological activities [6]. A chemical graph is a figurative representation of a compound according to its atomic features. These graphs may alternatively be expressed as a vector of categorical features, one such example being a SMILES string, with each element depicting the presence or absence of a chemical substructure or molecular property. Representing the compound in this way allows for the application of a range of machine learning techniques, including molecular data mining, compound diversity analysis, and compound activity prediction [16].

---

\*CONTACT A. Gosnell. [arrongosnelluk@aol.com](mailto:arrongosnelluk@aol.com)

Compounds are said to live within the chemical space, i.e., the space describing the ensemble of all organic chemical compounds [43]. A central principle of chemoinformatics is that neighbouring compounds, i.e., compounds close to one another within the chemical space, share similar properties [5]. The closeness, or distance, between compounds is typically measured using metrics on dichotomous feature spaces, with there being over 70 established methods for quantifying closeness in such feature spaces [12]. Among these, the Tanimoto similarity is the most widely used measure of closeness [3], and typically scores highest in terms of capturing the greatest level of intermolecular similarity [46, 53, 56]. The distance based on the Tanimoto similarity, known as the Tanimoto or Jaccard distance, is a proper metric [31], thereby satisfying the required metric criteria, in particular the triangle inequality.

The Tanimoto similarity has been widely incorporated in a range of machine learning applications for compound discovery and property prediction. In a regression setting, [39] developed mixed deep neural networks, which leveraged both chemical text (SMILES) as well as molecular descriptors (MACCS fingerprints) for predicting chemical properties, whilst [48] implemented random forests and deep neural networks to molecular property and reactivity prediction. Support vector machines [52] and Gaussian processes [35] have also been applied to molecular property prediction in a regression context. Furthermore, molecular fingerprints have been applied to a range of classification tasks. [4] implemented the molecular fingerprints of compounds, which inhibit cancer cell line growth within binary classification models. [55] applied convolutional neural networks and language-based models on molecular fingerprint data for several classification tasks. A notable criticism of these approaches is the absence of a scale parameter for controlling the strength of the similarity, thereby not properly accounting for its effect in the model.

Motivated by the aforementioned principle, in Section 2, we present a novel approach to incorporating chemical distance into Gaussian process (GP) models. The proposed GP model is defined on the chemical space, i.e., its inputs are the chemical compounds, while the values of the GP represent the effect of each compound on the outcome we wish to model. GPs are, however, commonly defined on Euclidean spaces, and are typically applied when modelling geographical phenomena. The metrics employed for analysing chemical structures are inherently non-Euclidean. Consequently, when modeling chemical structures, it is necessary to adapt the distance metric within the GP covariance. In Section 3 of this paper, we provide a mathematical framework to demonstrate that, indeed, GPs can be defined on non-Euclidean spaces, such as the chemical space, by incorporating the Tanimoto metric within the GP’s covariance structure. In addition, we present suitable isotropic correlation functions adapted to live on the chemical space. An important distinction between our proposed method and existing approaches is that we provide the GP kernels *with a scaling parameter*. To our knowledge, this is the first paper where such kernels based on the Tanimoto metric are developed. We focus on the case where the outcome is measured in an ordinal scale [1, 25, 34]. The proposed model can be described as a cumulative link model with correlated random effects [1, Section 5.1]. As the likelihood of the proposed model is not available in closed form, we apply Laplace’s method to approximate the likelihood and estimate the model parameters. This approach is described in Section 4. Thus, another contribution of this paper is the application of the Laplace approximation for estimation and prediction of ordinal data with Gaussian process random effects. Due to the correlation structure of the GP model, we can gain information from the effects of sampled compounds to predict the effect of unsampled compounds, a property which cannot be exploited with independent random effects, as well as provide uncertainty estimates of the proposed effects. The latter property makes GPs a particularly attractive choice to the application of drug discovery, especially when considering the cost-effectiveness of chemical production.

Exploration of the chemical space is vital for discovering new and effective compounds, and it is of particular interest to identify compounds that display high efficacy. Since the chemical

space encompasses an incredibly vast number of molecular structures, it is impossible to assess all configurations of molecular features to discover the ideal compound, making virtual screening particularly challenging. We, therefore, require optimisation techniques to automate discovery and propose interesting regions for further exploration. To that end, in Section 5, we develop a genetic algorithm, aided by the proposed model, to search over the chemical space and identify compounds of potentially high efficacy. We propose two optimality criteria that can be used for this purpose that are based on the features of the proposed model. The first criterion is based on maximising the probability that the outcome will belong to a given class, under given experimental conditions. On the other hand, it is not always possible to specify the experimental conditions, so our second criterion ignores the experimental conditions and focuses solely on the value of the GP.

Section 6 provides several simulation studies to demonstrate that the proposed method can recover the true parameter values, given the true model is the GP model with Tanimoto metric, as well as to demonstrate that the genetic algorithm can identify the optimal compound. Moreover, Section 7 applies the model to the practical scenario of hazard classification for organic solvents.

The computations presented in this paper were performed on a Windows 10 machine with an Intel Core i5-7300 CPU and 8GB RAM. The software R [40] was used for the implementation of the proposed model and the genetic algorithm, with the heavier computations implemented in Fortran 90. To conduct the analysis of the solvent data, the Python package RDKit [42] was used to derive each solvent’s daylight fingerprint from its SMILES code.

## 2 GP classification based on a cumulative probability model

We consider a chemical space  $\mathbb{C} = \{c_1, \dots, c_m\}$  of  $m$  distinct compounds. In practice,  $m$  is large, but only a small number of them will be used in experiments. We assume observed data  $(\mathbf{x}_1, y_1, c_{l_1}), \dots, (\mathbf{x}_n, y_n, c_{l_n})$ , where, for  $i = 1, \dots, n$ ,  $y_i \in \{1, 2, \dots, C\}$ , with  $1 < 2 < \dots < C$ , is the class response,  $\mathbf{x}_i \in \mathbb{R}^p$  are the testing conditions, and  $l_i \in \{1, \dots, m\}$  indicates the compound used in the  $i$ th experiment among the  $m$  distinct compounds in  $\mathbb{C}$ . The objective is to predict the outcome  $y_*$  given experimental conditions  $\mathbf{x}_*$  with compound  $c_*$ , i.e., to estimate the probabilities  $\Pr(y_* = j | \mathbf{y})$  for each class  $j \in \{1, \dots, C\}$ , where  $\mathbf{y} = (y_1, \dots, y_n)$ .

For modelling ordinal data, the cumulative link model [1, Section 5.1] is well-suited. Originally, this model has been proposed for independent observations, but has been extended by [14] to include a Gaussian process random effect. Our model follows the same approach, but considers more general link and correlation functions, that are suitable for chemical inputs.

Let  $T(\cdot, \cdot)$  represent the Tanimoto distance between pairs of compounds within the chemical space. We define  $u : \mathbb{C} \mapsto \mathbb{R}$  to be a GP on  $\mathbb{C}$ , such that for any finite collection of compounds  $\mathbf{u} = (u(c_1), \dots, u(c_m))$  is distributed according to the  $m$ -dimensional multivariate normal distribution with mean 0 and variance-covariance matrix  $K$ . We write the  $(r, s)$ th element of the matrix  $K$ , corresponding to compounds  $c_r$  and  $c_s$ , where  $r, s = 1, \dots, m$ , as  $k_{rs} = \sigma^2 R(T(c_r, c_s), \phi)$ , where  $\sigma^2$  denotes the variance parameter, and  $R(t, \phi)$  denotes the correlation function at distance  $t$  with scaling parameter  $\phi$ . Specific forms of  $R(t, \phi)$  are given in Section 3.

Let  $y$  denote the outcome of an arbitrary experiment under conditions  $\mathbf{x}$  with compound  $c$ , and let  $\gamma_j = \Pr(y \leq j | u(c))$ , with  $\gamma_C = 1$ . Our model assumes that

$$G(\gamma_j) = \eta_{jc} = \alpha_j + \beta^\top \mathbf{x} + u(c), \quad j = 1, \dots, C - 1, \quad (1)$$

where  $G : (0, 1) \mapsto \mathbb{R}$  is the link function,  $\beta \in \mathbb{R}^p$  denotes the regressor coefficients, and  $\alpha_1 < \dots < \alpha_{C-1}$  are the ordered intercepts.

Link functions model the non-linear effect of the regressor variables and the GP to the cumulative probabilities. Table 1 lists common choices of link functions that we consider in this paper, and, in

Link	$G(\gamma)$
Logit	$\log \frac{\gamma}{1-\gamma}$
Probit	$\Phi^{-1}(\gamma)$
Log-log	$\log(-\log(\gamma))$
C-log-log	$\log(-\log(1-\gamma))$

Table 1: Link functions within the proposed model, where  $\gamma$  are cumulative class probabilities and  $\Phi$  is the standard normal cumulative distribution function.

general, determine the predictive performance of the model. [15] showed that link misspecification can result in biased estimates and higher prediction error. In practice, a suitable link function should be chosen based on goodness-of-fit criteria, such as cross-validation, which we provide greater detail of in Section 7.

Let  $\gamma_{ij} = \Pr(y_i \leq j | u(c_{l_i}))$ ,  $j = 1, \dots, C$ , with  $\gamma_{iC} = 1$ , be the cumulative probabilities for up to class  $j$ , and  $\pi_{i1} = \gamma_{i1}$ ,  $\pi_{ij} = \gamma_{ij} - \gamma_{i,j-1}$ ,  $j = 2, \dots, C$  be the individual class probabilities. We assume that the distribution of each  $y_i$  is conditionally independent of  $y_{i'}$  for  $i' \neq i$  given  $u(c_{l_i})$ . Thus our model can be described by

$$\begin{aligned}
 y_i | u(c_{l_i}) &\stackrel{\text{ind}}{\sim} \text{Categorical}(\boldsymbol{\pi}_i), \quad i = 1, \dots, n, \\
 \mathbf{u} &\sim \text{N}_m(0, K),
 \end{aligned}
 \tag{2}$$

where  $\boldsymbol{\pi}_i = (\pi_{i1}, \dots, \pi_{iC})$  and  $\mathbf{u}$  is the value of the GP at the  $m$  distinct compounds.

The GP models are defined so that, if  $G(\cdot)$  is increasing, low values of  $u(c)$  correspond to high probabilities of an outcome in the highest class,  $C$ . To demonstrate this, we consider the odds ratio  $(1 - \gamma_j)/\gamma_j$ , for  $j = 1, \dots, C - 1$ , and its behaviour as a function of  $u(c)$ . We observe that  $(1 - \gamma_j)/\gamma_j = 1/\gamma_j - 1 = 1/G^{-1}(\eta_{jc}) - 1$ , where  $\eta_{jc} = \alpha_j + \beta^\top \mathbf{x} + u(c)$ . Therefore, if  $G$  is an increasing function, then so is  $G^{-1}$ , and in that case, the odds ratio of observing a class higher than  $j$  is a decreasing function of  $u(c)$ .

### 3 Fingerprints as a representation of the chemical space

Chemical fingerprints are a widely used concept in the analysis between molecular substructures and biological activities. Fingerprints are typically represented as  $\kappa$ -dimensional bit vectors, with the features being based on their chemical composition, or graph. Each feature within the fingerprint indicates the presence of atomic substructures, such as functional groups, ring systems, or atom arrangements. For example, a fingerprint might have a bit set to 1 if a certain functional group (like a hydroxyl group) is present within the molecule. Figure 1 illustrates two simple molecules and their associated fingerprints. We observe that the two molecules share a common ring. Similarity measures, such as the Tanimoto similarity, capture the intersection of molecular properties of chemical compounds through a similarity score.

The Tanimoto similarity is a measure of closeness between chemical compounds. In defining the Tanimoto similarity, consider a collection of bit vectors of the form  $c_r = (c_{r1}, c_{r2}, \dots, c_{r\kappa})$ , where  $c_{ri}$  is either 0 or 1, and not all 0, denoting the presence of feature (atomic substructure)  $i$  in the  $r$ th compound,  $i = 1, \dots, \kappa$ . The Tanimoto similarity  $S_{rs} = S(c_r, c_s)$ , for a pair of compounds  $c_r, c_s$ , is

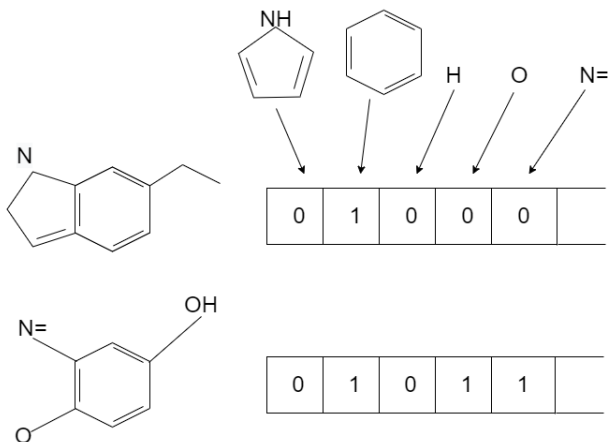


Figure 1: Two molecules and their corresponding fingerprints based on their substructures. The second feature within the two fingerprints has the value of 1, indicating the common presence of the corresponding substructure.

defined to be the number of features in common between the two compounds over the number of features in either. More specifically,

$$S_{rs} = \frac{\langle c_r, c_s \rangle}{\langle c_r, c_r \rangle + \langle c_s, c_s \rangle - \langle c_r, c_s \rangle}, \quad (3)$$

where  $\langle c_r, c_s \rangle = \sum_{i=1}^{\kappa} c_{ri}c_{si}$ . By definition,  $0 \leq S_{rs} \leq 1$ . When the two compounds have no features in common, their Tanimoto similarity is zero, i.e.,  $S_{rs} = 0$ , and when the compounds have identical features, their Tanimoto similarity is 1, i.e.,  $S_{rs} = 1$ .

An important result that justifies the use of the Tanimoto similarity as a correlation matrix of the GP is that the  $m \times m$  matrix  $S$  with elements  $S_{rs}$ ,  $r, s = 1, \dots, m$ , is positive definite [9, 22].

Subtracting the Tanimoto similarity from 1 converts it into a distance [21, 23], with the Tanimoto distance between compounds  $c_r$  and  $c_s$  denoted

$$T(c_r, c_s) = T_{rs} = 1 - S_{rs}.$$

Some authors [20] used the Tanimoto distance directly within a Gaussian kernel to model the correlation of a Gaussian process. Although the Tanimoto distance is a metric, it is non-Euclidean, and can produce non-positive definite correlations when used with spatial kernels [13].

As an example, consider the chemical space  $\mathbb{C} = \{c_1 = (0, 1, 1), c_2 = (1, 0, 1), c_3 = (1, 1, 0), c_4 = (1, 1, 1)\}$ . The matrix of pairwise Tanimoto distances,  $T$ , and the corresponding correlation matrix  $R$  with elements  $R_{rs} = \exp(-T_{rs}^2)$ , are given by

$$T = \begin{pmatrix} 0 & 2/3 & 2/3 & 1/3 \\ & 0 & 2/3 & 1/3 \\ & & 0 & 1/3 \\ & & & 0 \end{pmatrix}, \quad R = \begin{pmatrix} 1 & 0.6412 & 0.6412 & 0.8948 \\ & 1 & 0.6412 & 0.8948 \\ & & 1 & 0.8948 \\ & & & 1 \end{pmatrix} \text{ to 4 decimal points.}$$

Note that the distances given in  $T$  cannot correspond to distances in some Euclidean space. To see this, suppose there exist points  $\varepsilon_1, \dots, \varepsilon_4$  on some Euclidean space with pairwise distances given by  $T$ . Then, as  $T_{14} + T_{24} = T_{12}$ ,  $T_{14} + T_{34} = T_{13}$ , and  $T_{24} + T_{34} = T_{23}$ , the point  $\varepsilon_4$  must lie simultaneously in the middle of the edges of the equilateral triangle formed by  $\varepsilon_1$ ,  $\varepsilon_2$ , and  $\varepsilon_3$ , which

Correlation	$R(t, \phi)$
independent	$\mathbb{1}(t = 0)$
exponential	$\exp\{-\sqrt{t}/\phi\}$
Gaussian	$\exp\{-t/\phi^2\}$
Tanimoto	$1 - t$

Table 2: Correlation functions based on the Tanimoto metric at distance  $t$  with scaling parameter  $\phi$ .

is impossible. Note also that the correlation matrix  $R$  is not positive definite as its lowest eigenvalue is about  $-0.036$ .

Next, we discuss the use of the Tanimoto distance with well-known spatial kernels.

**Definition 1.** Let  $(\mathbb{C}, d)$  be a metric space. The metric  $d$  is called Euclidean if for any set of points  $c_1, \dots, c_m \in \mathbb{C}$ , there exist  $\varepsilon_1, \dots, \varepsilon_m \in \mathbb{R}^\alpha$  ( $\alpha$  depends on  $m$ ), such that  $d(c_r, c_s) = \|\varepsilon_r - \varepsilon_s\|$  for all  $r, s = 1, \dots, m$ , where  $\|\cdot\|$  denotes the Euclidean norm in  $\mathbb{R}^\alpha$ . In this case, we say that the points  $\{c_1, \dots, c_m\}$  can be isometrically embedded in a Euclidean space of dimension  $\alpha$ .

As an example, any three points,  $c_1, c_2, c_3$ , with pairwise distances  $d_{ij} = d(c_i, c_j)$ ,  $i < j \in \{1, 2, 3\}$  can always be embedded in a 2-dimensional Euclidean space, where the embedded points  $\varepsilon_1, \varepsilon_2, \varepsilon_3$  correspond to the vertices of a triangle with side lengths  $d_{12}, d_{13}, d_{23}$ .

The following theorem, appearing in [24], can be used to show that a metric is Euclidean. We denote the  $m \times m$  identity matrix by  $I_m$ , and the  $m \times m$  matrix of ones by  $J_m$ .

**Theorem 1.** Let  $(\mathbb{C}, d)$  be a metric space.

1. The metric  $d$  is Euclidean if and only if, for any set of points  $c_1, \dots, c_m \in \mathbb{C}$ , the  $m \times m$  matrix  $B = HAH$  is positive semi-definite, where  $H = I_m - m^{-1}J_m$ , and  $A$  is the  $m \times m$  matrix with elements  $A_{rs} = -d(c_r, c_s)^2/2$ ,  $r, s = 1, \dots, m$ .
2. Furthermore, let  $\alpha = \text{rank}(B)$ . Then, the points  $\{c_1, \dots, c_m\}$  can be isometrically embedded in a Euclidean space of dimension  $\alpha$ , and  $\alpha$  is the lowest dimension for which this is possible.

Now consider the chemical space  $\mathbb{C} = \{c_1, \dots, c_m\}$  with the metric  $d(c_r, c_s) = \sqrt{T(c_r, c_s)}$ . The matrix  $B$  from Theorem 1 is  $B = -\frac{1}{2}H(J_m - S)H = \frac{1}{2}HSH$ , where  $S$  is the  $m \times m$  matrix with elements given by (3). As  $S$  is positive definite,  $B$  is positive semi-definite and  $\text{rank}(B) = m - 1$ , therefore, the points  $\mathbb{C}$  can be embedded in a  $(m - 1)$ -dimensional Euclidean space. [33, Section 14.2.2] provide an algorithm for finding the points  $\varepsilon_1, \dots, \varepsilon_m$  in the Euclidean space. In the example given earlier,  $\varepsilon_1 = (-1/\sqrt{6}, -1/\sqrt{18}, -1/12)$ ,  $\varepsilon_2 = (1/\sqrt{6}, -1/\sqrt{18}, -1/12)$ ,  $\varepsilon_3 = (0, 2/\sqrt{18}, -1/12)$ ,  $\varepsilon_4 = (0, 0, 1/4)$  have pairwise Euclidean distances given by the square root of the elements of  $T$ .

This result allows us to create a vast catalogue of isotropic correlation functions using the Tanimoto distance, based on the correlation functions used in the GP literature, which allow the GP model to have certain properties. Table 2 lists several choices of the GP correlation,  $R(t, \phi)$ , corresponding to compounds with Tanimoto distance  $t$ . The independent correlation corresponds to what is commonly referred to as the mixed effects model, and is used for reference to assess the improvement when incorporating correlation.

## 4 Methodology

Our two primary objectives are to estimate the model parameters, obtained through maximising the model likelihood, and to estimate the probability an experiment falling within each ordered class, based on the available data. The model parameters are estimated first via the maximum likelihood method. The estimates are then used to construct the predictive distribution for the GP corresponding to a future experiment and compute the probabilities of each outcome.

The likelihood of the model, as well as the class probabilities for the given data, can be written only as multidimensional integrals with no closed-form expression. Techniques based on Monte-Carlo approximations of the likelihood, such as Monte-Carlo expectation maximisation [37], can be used. However, these methods lack computational efficiency and, given the high dimension of the GP, alternative methods are preferred. Therefore, we propose the use of Laplace approximation to compute the likelihood.

The size of the data in relation to the dimension of the GP is an important consideration when using Laplace approximation on binary data, first examined by [49]. In particular, the sample size  $n$  should increase at a higher rate than the dimension of the GP,  $m$ . Theoretically speaking,  $m$  is bounded above by  $2^\kappa$ , where  $\kappa$  denotes the number of features in the fingerprint vector. However, in finite samples,  $m$  can be comparable with  $n$ , so care must be taken when using our proposed method. Furthermore,  $\kappa$  can potentially increase as more compounds are added to the database as more features are needed to properly distinguish the compounds and ensure a rich representation of the space.

### 4.1 Estimation of model parameters

Let  $\theta = (\alpha_1, \dots, \alpha_{C-1}, \beta, \sigma^2, \phi)$  denote the model parameters. We use the symbol  $f(\cdot)$  to represent the probability density/mass function of the expression in the brackets. Given the model in (2), and excluding any factors that do not depend on  $\theta$  or  $\mathbf{u}$ , we have

$$f(\mathbf{y}|\mathbf{u}; \theta) \propto \prod_{i=1}^n \prod_{j=1}^C \pi_{ij}^{\mathbb{1}(y_i=j)}, \quad (4)$$

$$f(\mathbf{u}; \theta) \propto |K|^{-1/2} \exp\left(-\frac{1}{2} \mathbf{u}^\top K^{-1} \mathbf{u}\right),$$

where  $\mathbb{1}(\cdot)$  denotes the indicator function. The likelihood, based on data  $\mathbf{y}$ , is then

$$L(\theta|\mathbf{y}) = f(\mathbf{y}; \theta) = \int f(\mathbf{y}|\mathbf{u}; \theta) f(\mathbf{u}; \theta) d\mathbf{u}. \quad (5)$$

As noted earlier, the integral in (5) does not have a closed-form solution, so obtaining the maximum likelihood estimates of  $\theta$  by direct maximisation of the likelihood is not possible. To compute the likelihood, we apply the Laplace approximation, a technique which enables approximations to integrals of the form  $\int e^{-g(\mathbf{u})} d\mathbf{u}$ . Letting  $g(\mathbf{u}) = -\log[f(\mathbf{y}|\mathbf{u}; \theta) f(\mathbf{u}; \theta)]$ , we may express the second order Taylor expansion of  $g(\mathbf{u})$  as

$$g(\mathbf{u}) \approx g(\hat{\mathbf{u}}) + \frac{1}{2} (\mathbf{u} - \hat{\mathbf{u}})^\top \hat{H} (\mathbf{u} - \hat{\mathbf{u}}), \quad (6)$$

where  $\hat{\mathbf{u}}$  denotes the point at which the function  $g(\mathbf{u})$  is minimised, and  $\hat{H}$  denote the Hessian matrix of  $g(\mathbf{u})$  at  $\hat{\mathbf{u}}$ . By substituting (6) into (5), we obtain the approximation to the log-likelihood (up to a constant)

$$\log L(\theta|\mathbf{y}) \approx -g(\hat{\mathbf{u}}) - \frac{1}{2} \log |\hat{H}|. \quad (7)$$

Therefore,  $\hat{\theta}$  may be obtained by minimising (7) with respect to  $\theta$ . Let  $\mathcal{J}(\theta, \mathbf{y})$  denote the negative Hessian matrix of (7). Then,  $\mathcal{J}(\hat{\theta}, \mathbf{y})^{-1}$  is an estimate of the variance-covariance matrix of  $\hat{\theta}$ . Furthermore, recognising that  $f(\mathbf{u}|\mathbf{y}) \propto \exp\{-g(\mathbf{u})\}$ , which from (6) is proportional to a multivariate normal density, leads to the approximation

$$\mathbf{u}|\mathbf{y} \sim N_m(\hat{\mathbf{u}}, \hat{H}^{-1}) \text{ approximately as } n \rightarrow \infty. \quad (8)$$

## 4.2 Detailed derivations

The logarithm of the probability mass function for  $\mathbf{y}|\mathbf{u}$ , from (4), is given by

$$\begin{aligned} \ell(\mathbf{y}|\mathbf{u}; \theta) &= \sum_{i=1}^n \sum_{j=1}^C \mathbb{1}(y_i = j) \log(\pi_{ij}) \\ &= \sum_{i=1}^n \sum_{j=1}^C \mathbb{1}(y_i = j) \log(\gamma_{ij} - \gamma_{i,j-1}) \\ &= \sum_{i=1}^n \sum_{j=1}^C \mathbb{1}(y_i = j) \log(G(\eta_{i,j}) - G(\eta_{i,j-1})) \end{aligned}$$

where  $\eta_{i,j} = \alpha_j + \beta^\top \mathbf{x} + u(c_i)$ , and we define  $\alpha_0 = -\infty$ ,  $\gamma_{i,0} = 0$ . Therefore

$$\begin{aligned} \frac{\partial \ell}{\partial u(c)} &= \sum_{i=1}^n \sum_{j=1}^C \mathbb{1}(y_i = j) \mathbb{1}(c_i = c) b'_{ij}, \\ \frac{\partial^2 \ell}{\partial u(c) \partial u(c')} &= \sum_{i=1}^n \sum_{j=1}^C \mathbb{1}(y_i = j) \mathbb{1}(c_i = c) \mathbb{1}(c_i = c') (b''_{ij} - b'_{ij} b'_{ij}), \end{aligned}$$

where

$$b'_{ij} = \begin{cases} \frac{G'(\eta_{i,j})}{G(\eta_{i,j})}, & \text{if } j = 1, \\ \frac{G'(\eta_{i,j}) - G'(\eta_{i,j-1})}{G(\eta_{i,j}) - G(\eta_{i,j-1})}, & \text{if } j = 2, \dots, C-1, \\ \frac{-G'(\eta_{i,j-1})}{1 - G(\eta_{i,j-1})}, & \text{if } j = C, \end{cases}$$

$$b''_{ij} = \begin{cases} \frac{G''(\eta_{i,j})}{G(\eta_{i,j})}, & \text{if } j = 1, \\ \frac{G''(\eta_{i,j}) - G''(\eta_{i,j-1})}{G(\eta_{i,j}) - G(\eta_{i,j-1})}, & \text{if } j = 2, \dots, C-1, \\ \frac{-G''(\eta_{i,j-1})}{1 - G(\eta_{i,j-1})}, & \text{if } j = C. \end{cases}$$

Overall, we can write

$$\frac{\partial \ell}{\partial \mathbf{u}} = P^\top \Psi_1, \quad \frac{\partial^2 \ell}{\partial \mathbf{u} \partial \mathbf{u}^\top} = P^\top \Psi_2 P$$

where  $P$  is an  $n \times m$  binary matrix where its  $i^{\text{th}}$  row is 0 everywhere except at  $l_i$  which equals 1,



and  $\Psi_1$  is an  $n$ -dimensional vector and  $\Psi_2$  is an  $n \times n$  diagonal matrix with elements

$$\begin{aligned}\Psi_{1i} &= \sum_{j=1}^C \mathbb{1}(y_i = j) b'_{ij}, \\ \Psi_{2ii} &= \sum_{j=1}^C \mathbb{1}(y_i = j) (b''_{ij} - b'_{ij} b'_{ij}),\end{aligned}$$

respectively, for  $i = 1, \dots, n$ . To find  $\hat{\mathbf{u}}$  used in the Laplace approximation, we solve

$$K^{-1} \hat{\mathbf{u}} - P^\top \hat{\Psi}_1 = 0, \quad (9)$$

and the Hessian is  $\hat{H} = K^{-1} - P^\top \hat{\Psi}_2 P$ , where  $\hat{\Psi}_1$  and  $\hat{\Psi}_2$  denote  $\Psi_1$  and  $\Psi_2$  evaluated at  $\hat{\mathbf{u}}$ .

### 4.3 Prediction

The approximation in (8) enables the prediction of a class damage,  $y_*$ , for an untested compound,  $u_*$ . We begin by evaluating the conditional distribution  $u_* | \mathbf{y}$  to estimate the unobserved effects of the GP. Using the conditional independence of  $u_*$  and  $\mathbf{y}$  given  $\mathbf{u}$ , we observe that

$$f(u_* | \mathbf{y}) = \int f(u_* | \mathbf{u}) f(\mathbf{u} | \mathbf{y}) d\mathbf{u} \approx \int f(u_* | \mathbf{u}) \hat{f}(\mathbf{u} | \mathbf{y}) d\mathbf{u} =: \hat{f}(u_* | \mathbf{y}),$$

so the density  $f(u_* | \mathbf{y})$  can be approximated by a Gaussian density  $\hat{f}(u_* | \mathbf{y})$ , whose mean and variance can be computed using the law of total expectation and variance. In doing so,

$$\begin{aligned}\mathbb{E}[u_* | \mathbf{y}] &= \mathbb{E}[\mathbb{E}[u_* | \mathbf{u}] | \mathbf{y}] \\ &= \mathbb{E}[K_* K^{-1} \mathbf{u} | \mathbf{y}] \\ &= K_* K^{-1} \hat{\mathbf{u}}\end{aligned} \quad (10)$$

$$\begin{aligned}\text{Var}[u_* | \mathbf{y}] &= \mathbb{E}[\text{Var}[u_* | \mathbf{u}] | \mathbf{y}] + \text{Var}[\mathbb{E}[u_* | \mathbf{u}] | \mathbf{y}] \\ &= \mathbb{E}[K_{**} - K_*^\top K^{-1} K_* | \mathbf{y}] + K_*^\top K^{-1} \text{Var}[\mathbf{u} | \mathbf{y}] K_* K^{-1} \\ &= K_{**} - K_*^\top K^{-1} K_* + K_*^\top K^{-1} \hat{H}^{-1} K_* K^{-1},\end{aligned} \quad (11)$$

where  $K_* = \text{Cov}(\mathbf{u}, u_*)$ , and  $K_{**} = \text{Cov}(u_*, u_*)$ . Here, we have made use of the well-known relations  $\mathbb{E}[u_* | \mathbf{u}] = K_* K^{-1} \mathbf{u}$  and  $\text{Var}[u_* | \mathbf{u}] = K_{**} - K_*^\top K^{-1} K_*$  from Gaussian conditioning rules.

Let  $y_*$  denote the outcome of a future experiment under conditions  $\mathbf{x}_*$  using compound  $c_*$ . To obtain the predicted outcome, we require the probabilities  $\Pr(y_* = j | \mathbf{y})$  for  $j = 1, \dots, C$ . These can be estimated as follows.

$$\begin{aligned}\Pr(y_* = j | \mathbf{y}) &= E[\mathbb{1}(y_* = j) | \mathbf{y}] \\ &= E[E[\mathbb{1}(y_* = j) | \mathbf{y}, u_*] | \mathbf{y}] \\ &= E[E[\mathbb{1}(y_* = j) | u_*] | \mathbf{y}] \\ &= E[\pi_{*j} | \mathbf{y}] \\ &= \int \pi_{*j} f(u_* | \mathbf{y}) du_* \\ &\approx \int \pi_{*j} \hat{f}(u_* | \mathbf{y}) du_*.\end{aligned} \quad (12)$$

Equation (12) is evaluated using numerical integration. In this paper, we use the Gauss-Hermite quadrature method [17] with 21 integration points. In fact, under the probit link, the integral in (12) has an analytical expression (see Appendix A), however this is not the case for general link functions.

#### 4.4 Variance corrections to parameter uncertainty

The formula for  $\text{Var}[u_*|\mathbf{y}]$  given in (11) is a function of the model parameters,  $\theta$ . In practice,  $\theta$  is unknown and is replaced by its estimate  $\hat{\theta}$ , effectively assuming that the true value of  $\theta$  is  $\hat{\theta}$ . This ignores the uncertainty in the value of  $\theta$ . [7] provided a correction to the prediction variance for generalised linear mixed models with *independent* random effects. We follow a similar approach here to derive variance corrections to the GP estimates for our model.

Let  $u_*$  be the true value and let  $\hat{\mathbf{u}}_*(\mathbf{y}, \theta) = \mathbb{E}[u_*|\mathbf{y}]$  be the prediction with known  $\theta$ . We want to assess the error  $\hat{\mathbf{u}}_*(\mathbf{y}, \hat{\theta}) - u_*$ , where  $\hat{\theta}$  denotes the maximum likelihood estimator for  $\theta$ .

We write  $\hat{\mathbf{u}}_*(\mathbf{y}, \hat{\theta}) - u_* = \hat{\mathbf{u}}_*(\mathbf{y}, \hat{\theta}) - \hat{\mathbf{u}}_*(\mathbf{y}, \theta) + \hat{\mathbf{u}}_*(\mathbf{y}, \theta) - u_* = e_1 + e_2$ , where  $e_1 = \hat{\mathbf{u}}_*(\mathbf{y}, \hat{\theta}) - \hat{\mathbf{u}}_*(\mathbf{y}, \theta)$  is the additional error due to the uncertainty in  $\theta$  and  $e_2 = \hat{\mathbf{u}}_*(\mathbf{y}, \theta) - u_*$  is the error had  $\theta$  been known. Note that,  $e_1$  is a function of  $\mathbf{y}$ , but not of  $u_*$ , and  $\mathbb{E}[e_2|\mathbf{y}] = \hat{\mathbf{u}}_*(\mathbf{y}, \theta) - \mathbb{E}[u_*|\mathbf{y}] = 0$ . Then,

$$\begin{aligned}\mathbb{E}[e_1 e_2] &= \mathbb{E}[\mathbb{E}[e_1 e_2|\mathbf{y}]] \\ &= \mathbb{E}[e_1 \mathbb{E}[e_2|\mathbf{y}]] = 0.\end{aligned}$$

Furthermore,

$$\begin{aligned}e_1 &= \hat{\mathbf{u}}_*(\mathbf{y}, \hat{\theta}) - \hat{\mathbf{u}}_*(\mathbf{y}, \theta) \\ &\approx \nabla_{\theta} \hat{\mathbf{u}}_*(\mathbf{y}, \theta)^{\top} (\hat{\theta} - \theta) \\ \Rightarrow \text{Var}(e_1) &\approx \nabla_{\theta} \hat{\mathbf{u}}_*(\mathbf{y}, \theta)^{\top} \mathcal{I}(\theta)^{-1} \nabla_{\theta} \hat{\mathbf{u}}_*(\mathbf{y}, \theta),\end{aligned}$$

where  $\mathcal{I}(\theta)$  denotes the Fisher information matrix of  $\theta$ , which can be estimated by  $\mathcal{J}(\hat{\theta}, \mathbf{y})$ . Then,

$$\begin{aligned}\mathbb{E}[(\hat{\mathbf{u}}_*(\mathbf{y}, \hat{\theta}) - u_*)^2] &= \mathbb{E}[(e_1 + e_2)^2] \\ &= \text{Var}(e_1 + e_2) \\ &= \text{Var}(e_1) + \text{Var}(e_2) \\ &\approx \nabla_{\theta} \hat{\mathbf{u}}_*(\mathbf{y}, \theta)^{\top} \mathcal{I}(\theta)^{-1} \nabla_{\theta} \hat{\mathbf{u}}_*(\mathbf{y}, \theta) + \text{Var}[u_*|\mathbf{y}].\end{aligned}\tag{13}$$

The second term in (13) is given by (11), while the first term is the variance correction due to estimation in  $\theta$ . To compute the derivatives  $\nabla_{\theta} \hat{\mathbf{u}}_*(\mathbf{y}, \theta)$ , note that, by (10),  $\nabla_{\theta} \hat{\mathbf{u}}_*(\mathbf{y}, \theta) = K_* K_*^{-1} \nabla_{\theta} \hat{\mathbf{u}}(\mathbf{y}, \theta)$ , where  $\hat{\mathbf{u}}(\mathbf{y}, \theta)$  is the solution to (9). By differentiating both sides of (9) with respect to elements of  $\theta$ , we are able to compute  $\nabla_{\theta} \hat{\mathbf{u}}(\mathbf{y}, \theta)$  algebraically.

#### 4.5 A note on computational complexity

The proposed methodology can be summarised in two steps.

1. Estimation of the parameters  $\theta$  by maximising (7).
2. Calculation of class probabilities via (12) based on the estimates obtained.

Parameter estimation involves the use of a numerical optimisation procedure, such as the quasi-Newton algorithm and construction of the Laplace approximation at each iteration. The Laplace approximation itself requires solving (9), which consists of a separate quasi-Newton iteration procedure. In our experience, only few iterations of the inner optimisation are required, however, each iteration involves an inversion of an  $m \times m$  dense matrix, which has computational complexity in the order of  $O(m^3)$ . Thus, denoting the average number of iterations for maximising (7) by  $L_1$ , and the average number of iterations for solving (9) by  $L_2$ , then the average complexity of the first step is  $O(L_1 L_2 m^3)$ .

The prediction step involves calculation of the predictive mean and variance given by (10) and (11) respectively. The matrices  $K^{-1}$  and  $H^{-1}$  would be available during the estimation step, so the computational complexity in this case would be linear in  $m$ ,  $O(m)$ .

## 5 A genetic algorithm for drug-discovery

A fundamental aspect of chemoinformatics is the ability to identify promising compounds without the requirement of physical testing. Due to the expanse of the chemical space and the high dimensionality of the molecular representation, assessing the performance of every compound is currently impractical. Therefore, efficient search methods are required to guide exploration of the chemical space and propose interesting regions for further analysis.

In pursuit of the above objective, we advocate for the utilisation of a genetic algorithm. Genetic algorithms are a family of stochastic optimisation techniques inspired by the Darwinian model of natural selection [50]. They are particularly effective in the application of feature selection [10, 27]. The two defining characteristics of a genetic algorithm are the crossover and mutation rates. The crossover rate mirrors the natural process of genetic inheritance, as it involves passing on a portion of genes from each parent to the offspring population. Conversely, the mutation rate introduces randomness into the population, mimicking the occasional genetic variations observed in evolutionary cycles. Within each iteration of the algorithm, a generation of compounds reproduce, resulting in an offspring population. The performance of the offspring population is evaluated through a fitness score. Features associated with higher fitness scores are more likely to be passed down to subsequent generations during the reproductive cycle. After a fixed number of reproductive cycles, the features associated with the highest fitness scores form the fittest individuals in the population.

To demonstrate the genetic algorithm, consider a population of an even number of compounds,  $k$ , denoted  $\{c_1, \dots, c_k\}$ , along with their corresponding fitness, defined below, where each compound is represented by its fingerprint vector  $c_r = (c_{r1}, \dots, c_{r\kappa})$ , for the  $r$ th compound,  $r = 1, \dots, k$ . We then perform the following steps iteratively. Each step produces an updated population, which we also denote by  $\{c_1, \dots, c_k\}$ .

**Selection** Each compound is ranked according to the number of compounds with fitness lower than that compound’s fitness. The population of compounds is then updated by sampling  $k$  elements with replacement among  $\{c_1, \dots, c_k\}$ , with the probability of choosing a particular compound, say  $c_r$ , being proportional to  $a + b\rho_r$ , where  $a, b > 0$  are chosen parameters of the algorithm, and  $\rho_r$  is the rank of the  $r$ th compound.

**Crossover** We form  $k/2$  pairs  $(c_r, c_{r+1})$  for  $r = 1, 3, \dots, k-1$ . For each pair, we perform crossover with probability  $p_c$ . We sample an index  $\lambda$  uniformly in  $\{1, \dots, \kappa\}$ . Then, we update

- $c_{r,i} \leftarrow c_{r,i}$  and  $c_{r+1,i} \leftarrow c_{r+1,i}$ , for  $i \leq \lambda$ , and
- $c_{r,i} \leftarrow c_{r+1,i}$  and  $c_{r+1,i} \leftarrow c_{r,i}$ , for  $i > \lambda$ .

**Mutation** For each compound,  $c_r$ , we perform mutation with probability  $p_m$ . We sample an index  $\delta$  uniformly in  $\{1, \dots, \kappa\}$ . Then, we update  $c_{r\delta} \leftarrow 1 - c_{r\delta}$ .

In terms of fitness value, suppose that we are interested in identifying the compound  $c_*$  that is more likely to lead to an outcome  $y_*$  in the highest class, for given experimental conditions,  $\mathbf{x}_*$ , under the current data  $\mathbf{y}$ . According to our model, this is achieved by the compound with the highest value of  $\Pr(y_* = C|\mathbf{y})$ , which is estimated by (12) for  $j = C$ . This objective may be

desirable if the experimental conditions have been decided. An alternative objective can be to find the compound with the lowest GP mean, given by (10). This is interpreted as finding the compound that is most likely to correspond to the lowest GP value, and therefore, the highest probability for the highest class, regardless of the experimental conditions. The additional benefit of this objective is that it avoids the numerical integration for computing the class probabilities.

A crucial part of the methodology is the use of the prediction formula (12) to determine the fitness of a compound. It is therefore imperative that the predictions are accurate. In practice it is possible to test only few compounds which then form the data used to fit the model. In such cases, these compounds must be selected from a large data base in a way that they form a representative sample of the chemical space. There are several approaches used in the literature for this purpose including clustering, dissimilarity-based, cell-based, and optimisation approaches [see 29, Chapter 6 for a review]. [19] studied optimality criteria with the goal of minimising the average prediction variance that can be applied here, while [45] proposed an algorithm that can be used for dissimilarity-based selection.

## 6 Simulation studies

We conducted various simulation studies to assess the performance of the proposed methods. The general model is described by equations (1) and (2), with specific choices for covariates and link functions as described below.

### 6.1 Estimation performance

In the first study, we consider estimation of the model parameters. The chemical space is formed by combining 5 features, producing a total of  $m = 2^5 - 1 = 31$  distinct compounds (excluding the compound with no active features). The data consist of  $n = 341$  experiments, where each of the 31 compounds was tested under 11 different experimental conditions. Let  $y_{ik}$ , where  $i = 1, \dots, 11$ , and  $k = 1, \dots, 31$ , denote the observed outcome at the  $i$ th experiment with compound  $k$ , which can be among  $C = 3$  categories. The model for the cumulative probabilities is

$$\text{logit Pr}(y_{ik} \leq j) = \alpha_j + \beta x_i + u_k, \quad j = 1, 2,$$

with a single covariate  $x_i = (i - 1)/10$ . We consider two different GP models for  $\mathbf{u}$ , one using the Gaussian covariance, and one using the exponential covariance, both with variance parameter  $\sigma^2$  and scale parameter  $\phi$ . The model parameters  $\alpha_1$ ,  $\alpha_2$ ,  $\beta$ ,  $\sigma^2$ , and  $\phi$  are considered unknown. We conducted two different simulation studies from each model with the true parameter values chosen as shown in Table 3. We performed 500 simulations in total from each model, where we estimate the parameters using the proposed method. Table 3 shows the average estimate across the 500 simulations of each parameter and for each model, in addition to the true and estimated standard deviations, based on the inverse of the Hessian matrix of the approximate log-likelihood. The results in Table 3 show that the proposed method can estimate the parameters accurately. In particular, for estimating the parameters  $\alpha_j$  and  $\beta$ , there is virtually no bias. In terms of estimating the standard deviation using the inverse of the Hessian matrix of the approximate log-likelihood, we observe that the proposed method underestimates the standard deviation slightly, except for the scale parameter  $\phi$  where the method overestimates the standard deviation. Figure 2 provides an overview of the parameter estimate distribution in the simulation studies, with the true parameter value indicated by a red "x". It is apparent that the estimates exhibit almost no bias (apart from the estimation of  $\phi$  in some cases), as the true value frequently lies near the median of the estimated

		Gaussian covariance			Exponential covariance			
True		Est	StDev	Est SD	Est	StDev	Est	StDev
$\alpha_1$	-1.0	-0.99	0.34	0.29	-0.99	0.41		0.28
$\alpha_2$	0.0	0.01	0.34	0.29	0.01	0.40		0.27
$\beta$	1.0	1.00	0.35	0.33	1.00	0.35		0.34
$\sigma^2$	0.5	0.44	0.28	0.22	0.38	0.26		0.22
$\phi$	0.5	0.44	0.40	0.96	0.31	0.50		2.18
$\alpha_1$	-0.5	-0.50	0.29	0.29	-0.49	0.29		0.30
$\alpha_2$	0.5	0.50	0.28	0.29	0.50	0.28		0.30
$\beta$	-1.0	-0.99	0.36	0.35	-0.99	0.36		0.35
$\sigma^2$	1.0	0.96	0.38	0.38	0.96	0.38		0.39
$\phi$	0.1	0.16	0.22	0.75	0.07	0.19		0.55

Table 3: Performance measures for estimation of the parameters. Showing the true parameter values, average estimates across all simulations, standard deviation of the estimates across all simulations, and average of the standard deviation estimates across all simulations.

Gaussian		Exponential	
U	C	U	C
0.0099	0.0011	0.0029	0.0002
0.1593	0.1211	0.1558	0.1111

Table 4: Average squared differences between the empirical variance and the uncorrected variance estimate (U) and between the empirical variance and the corrected variance estimate (C). The models are as in Table 3.

values. Overall, we can conclude that the proposed methodology provides accurate estimates and standard errors for the model parameters.

## 6.2 Assessment of the prediction variance formula

Next, we consider the accuracy of the variance correction formula (13). Using the simulated data from Section 6.1, we predict the GP value at the 31 compounds for each of the 500 simulated data sets. We then compute the empirical variance for the GP corresponding to each compound across the 500 simulations. We compare this against the average prediction variance estimate based on the uncorrected and corrected versions. Table 4 shows the average (over the 31 compounds) squared difference between the empirical variance and the uncorrected and corrected estimates. We observe that the corrected version is more accurate, and, in fact, examination of the individual estimates shows that the uncorrected version underestimates the variance. This verifies that the corrected prediction variance formula (13) is more accurate.

## 6.3 Assessment of the drug discovery algorithm

In the final simulation study we aim to assess the ability of the proposed genetic algorithm of Section 5 to identify compounds of high efficacy. We simulated from the same four models as in Section 6.1, except that the chemical space was increased to 10 features, i.e.  $2^{10} - 1 = 1023$  compounds (excluding the compound with no active features). In addition, only  $m = 90$  compounds were tested. These compounds were selected based on a space-filling criterion using the Euclidean distance  $d(\cdot, \cdot) = \sqrt{T(\cdot, \cdot)}$  [45]. After fitting the model to each generated data set, we use the

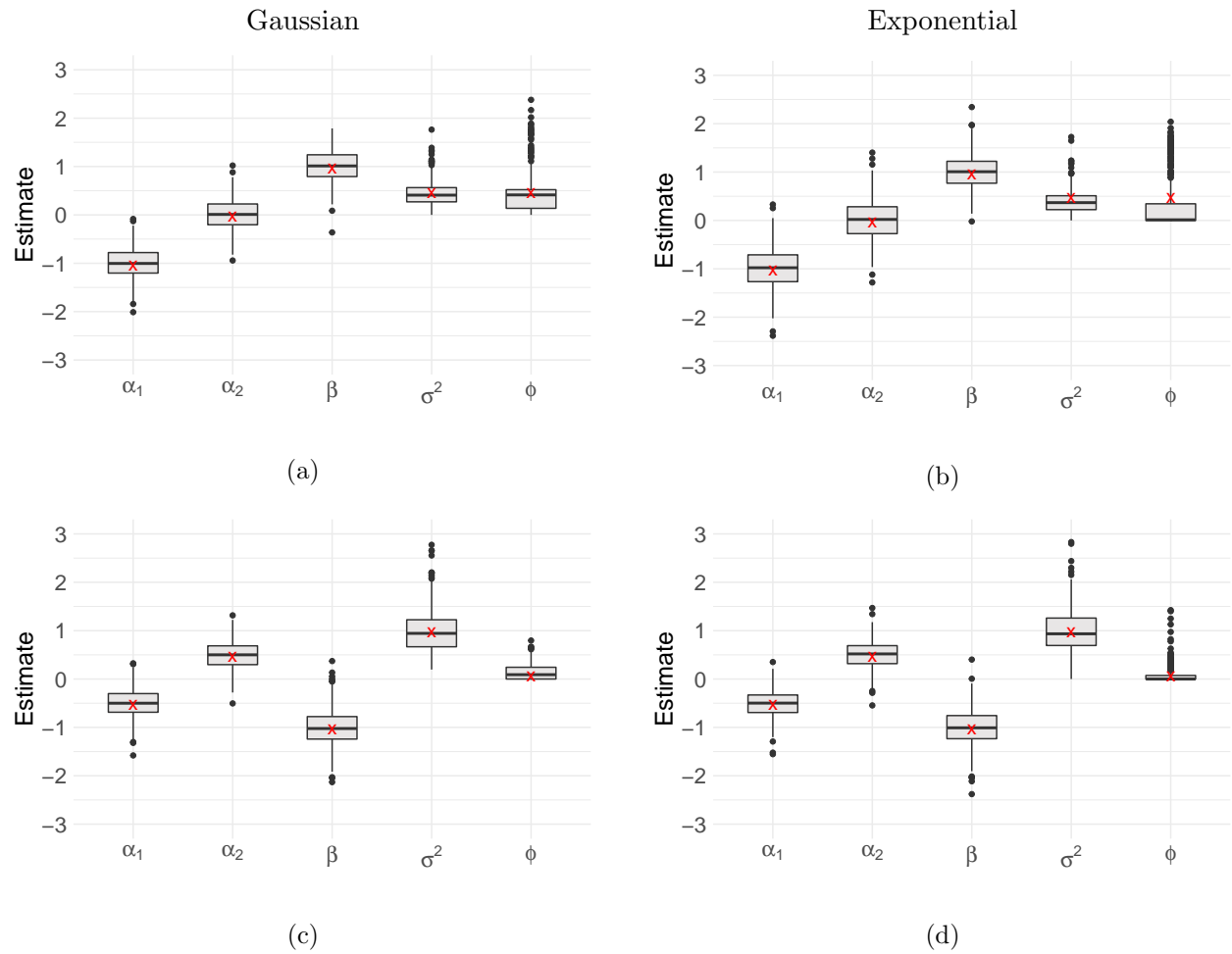


Figure 2: Showing the distribution of the estimated parameter values from the simulation studies. The logit link was used for all four studies. The true model parameters are indicated with a red x.

	Gaussian				Exponential			
	1	2	3	4+	1	2	3	4+
GP	73	19	6	2	65	26	5	4
Pr( $y = 3$ )	70	22	3	5	77	14	5	4
GP	75	15	7	3	76	11	5	8
Pr( $y = 3$ )	77	12	7	4	77	9	7	7

Table 5: Number of times that the compound returned by the genetic algorithm had each rank when the objective is to minimise the GP value (first and third rows), or maximise the probability in the third class with  $x = 1$  (second and fourth rows). The models are as in Table 3.

proposed genetic algorithm to find the compound that (a) corresponds to the lowest GP value, and (b) corresponds to the highest probability of an output in the third category when  $x = 1$ . The genetic algorithm was run with population size  $k = 10$ , for 100 generations, and with parameters  $a = 10$ ,  $b = 1$ ,  $p_c = 0.8$ , and  $p_m = 0.1$ . We applied this method to 100 generated data sets simulated from each of the four models. We then compared how highly ranked the derived compound is, compared to the truly optimal compound as predicted by the fitted model, i.e., we compute (10) and (12) for each of the 1023 compounds in our model, which we then rank from best to worst, and then find the rank that corresponds to the compound selected by the genetic algorithm. Table 5 shows how many times each rank was attained. On average, more than 70% of the time, the genetic algorithm returned the optimal compound, and more than 90% of the time it returned one of the top two compounds. Of course, the results can be improved by increasing the population size  $k$  and the number of iterations, with the additional computational cost. This suggests that the proposed algorithm works well for this problem.

## 7 Hazard classification of organic solvents

To illustrate the proposed GP model, we consider the list of 500 organic solvents published in [28]. The list contains a range of chemical information, including its classification according to the German water hazard class (WGK) [18], which classifies chemicals in three levels as slightly, obviously, and highly hazardous to water, in increasing severity. The other variables contained in the data set describe the properties of the solvents, which includes the GHS classification, GHS hazard statements, Hansen Solubility Parameter, boiling temperature, vapor pressure at atmospheric pressure, density, molecular weight, and molar volume. The SMILES-codes are also included, which illustrate the chemical graph of the molecule and are used to derive each solvent’s chemical fingerprint. After removing missing values,  $n = 485$  data points remain in the proportions of 25%, 22%, and 52% respectively for the three WGK ordered classes.

We consider the proposed ordinal model, given by equations (1) and (2), with a combination of correlation and link functions given in Table 2 and Table 1. In addition we fit a random forest model using the R package [30], which incorporates the chemical information provided in the data as predictors instead of the derived fingerprint vector.

Let  $\hat{\pi}_{kj}$  denote the estimated probability that the  $k$ th deleted outcome is  $j$ . If the realised outcome is  $y_k = j'$ , we define the logarithmic loss by  $L_{\log}(k) = -\log \hat{\pi}_{kj'}$ , and the spherical loss by  $L_{\text{sph}}(k) = -\hat{\pi}_{kj'} \left( \sum_{j=1}^C \hat{\pi}_{kj}^2 \right)^{-1/2}$ . We use 5 fold cross-validation to assess the performance of each model where approximately 20% of the observations from each class were randomly removed from the data in each fold and the models fitted on the remaining data. After fitting each model, we

Model	Logarithmic	Spherical	Time (s)
probit Tanimoto	0.904 (0.024)	-0.680 (0.014)	26.8
probit Gaussian	0.906 (0.023)	-0.679 (0.014)	36.5
logit Tanimoto	0.908 (0.023)	-0.679 (0.014)	24.4
C-log-log Tanimoto	0.911 (0.034)	-0.677 (0.021)	31.3
logit Gaussian	0.911 (0.022)	-0.677 (0.013)	35.5
log-log Tanimoto	0.917 (0.022)	-0.675 (0.013)	22.9
log-log Gaussian	0.920 (0.021)	-0.674 (0.013)	33.3
probit exponential	0.922 (0.018)	-0.673 (0.012)	33.1
random forest	0.927 (0.023)	-0.671 (0.010)	0.1
logit exponential	0.929 (0.018)	-0.670 (0.011)	29.0
log-log exponential	0.937 (0.019)	-0.665 (0.012)	30.4
C-log-log Gaussian	0.939 (0.025)	-0.666 (0.013)	32.9
C-log-log exponential	0.958 (0.018)	-0.658 (0.009)	39.1
log-log independent	1.020 (0.004)	-0.624 (0.002)	14.9
probit independent	1.020 (0.005)	-0.624 (0.003)	15.4
logit independent	1.023 (0.002)	-0.622 (0.001)	13.1
C-log-log independent	1.025 (0.019)	-0.624 (0.009)	18.0

Table 6: 5-fold cross validation results of the water hazard data. Showing the averaged mean and standard deviations of the models’ log and spherical scores, as well as the average time taken in seconds to maximise the approximate likelihood.

predict the outcome at the removed data from the solvent’s fingerprint (in the case of the ordinal model), or chemical information (in the case of the random forest model). The log and spherical losses were averaged across the five folds.

Table 6 shows the average cross-validation loss for each model. In addition to this, the average time to maximise the approximate likelihood is reported. We observe the model with probit link and Tanimoto covariance has the greatest performance, with an average time of 26.8 seconds. The models based on the independent correlation have the lowest scores, indicating the relevance of the fingerprint information. We also observe that most models generally perform better than the random forest model, suggesting the ordinal model is able to extract the necessary information from the solvent’s fingerprint when predicting the WGK class.

Next, we consider identifying which fingerprint features contribute the most to a solvent being classed as highly hazardous (class 3). We consider only those features that are present in more than 10% of the solvents in our data (177 features), with the remaining features fixed at 0. As an exploratory step, we find which features appear most frequently among the class-3 solvents; 3 features appear in more than 80% of the class-3 solvents, and 5 more appear in more than 70%. We then used the proposed genetic algorithm with population size  $k = 100$ , number of generations 500, and parameters  $a = 100$ ,  $b = 1$ ,  $p_c = 0.8$ , and  $p_m = 0.1$  to find which solvents are predicted to have the highest class-3 probability. We examine the features common to the 100 fittest members from the optimisation. Twenty features appeared in all members of the population, which includes the 3 most common among class-3 solvents in the data, and 2 of the 5 that appear more than 70% of the time. In addition, 32 features appear in at least half of the members of the population, which could be further investigated as potential drivers of hazardousness.

Referees of this paper have expressed concerns regarding the validity of the anisotropy assumption, which underpins the proposed methodology. Our case presents a challenge as techniques



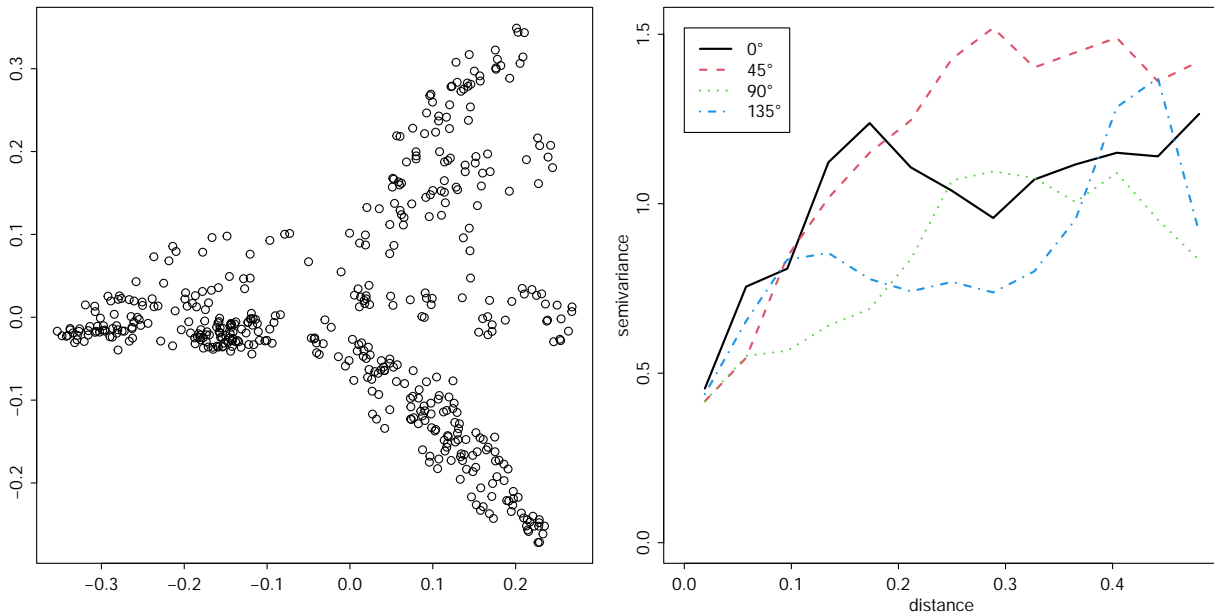


Figure 3: Left plot: Lower-dimensional embedding of the compound fingerprints for the data of Section 7. Right plot: Directional semi-variogram based on the lower-dimensional embedding for the same data.

designed to assess anisotropy in spatial data are not directly applicable due to the high dimensionality of the embedding space, and developing methodologies tailored to address this challenge extends beyond the scope of our paper. To investigate the issue, we consider a lower-dimensional embedding of the compound fingerprints to a Euclidean space of dimension 2 using multidimensional scaling [33]. Figure 3 (left) shows the lower-dimensional representation of the compounds in that space. This allows us to compute (using the R package `geoR` [44]) the directional semi-variogram of the predicted GP at various directions, which is shown in Figure 3. Each variogram in Figure 3 corresponds to one directional angle, with angles of 0, 45, 90, and 135 degrees. We observe the trajectories of the variograms are similar for the given directions, suggesting the absence of anisotropy. The conclusion drawn from this observation is that the isotropic assumption is reasonable for the proposed GP model. In other words, the spatial dependence in the data is consistent across different directions, supporting the use of an isotropic GP model.

## 8 Conclusion

The motivation for this paper is to provide rigorous statistical methodology for chemoinformatics with particular focus in predicting properties of chemical compounds and aiding drug discovery. We propose a GP model over the chemical space to capture the correlation in the effects of chemical compounds based on their chemical structure. The GP correlation is modelled in terms of the Tanimoto distance, which is a non-Euclidean metric on the chemical space. This approach allows us to incorporate compound similarity in our model, and implement the closeness principle of chemoinformatics.

Our findings show that the proposed GP model has better performance in the application considered over the independent random effects model and the random forest model, which demonstrates that, indeed, the correlation between compounds should be taken into account. In addition, we have

shown that the genetic algorithm is a suitable method for exploration of the chemical space, and can be used to propose compounds of great efficacy. Our simulation study validated the suitability of the proposed estimation techniques.

We focused on the case where the outcome is measured in an ordinal scale, although the model can be extended to the case where the outcome is categorical (for classification), or continuous (for regression). The change in the model for the classification task is that the link function is applied to the probabilities for each class instead of the cumulative probabilities. The derivations in this case would be similar. For the regression task, the multinomial distribution is replaced by a normal distribution, with a separate variance (noise) parameter. In this case, the model fitting process simplifies considerably as it is possible to derive the predictive distributions in closed form. We expect the proposed methodology to have similar performance in those cases.

A notable shortfall of our application is that all features within the chemical fingerprint are considered equally important. As each fingerprint consists of many features, examining each one individually would be time-consuming. A natural extension of the proposed approach is to embed the chemical space in a higher-dimensional Euclidean space to account for potential anisotropy or non-stationarity [8, 47]. Furthermore, the optimisation method is not guaranteed to produce a realistic compound, however this issue can be overcome by considering observable compounds that are similar to the one derived from the optimisation method. Another open question is the identification of important fingerprint features for prediction. One possible research direction towards that goal is the implementation of Shapley values in the spirit of [11].

The proposed model and techniques may be applied to other settings, such as predicting the potency of pharmaceutical products, and properties of food ingredients. Directions for future work are to implement sparse correlation functions that allow use of our methods to large chemical databases. Further analysis could also incorporate other metrics on the chemical space, such as the cosine similarity or the dice coefficient, as well as consider interaction effects between the GP and other covariates. Another interesting extension would be to consider alternative representations of the chemical space, such as those based on topological data analysis [54].

## A Prediction under the probit link

In this section we derive the closed-form expression for the prediction probabilities of a future experiment under the probit link. These probabilities can be expressed in integral form in general by the right-hand side of (12).

We will make use of the following lemma, which is proven in Section 3.9 of [41].

**Lemma 1.** *Let  $f(z|\mu, \sigma^2)$  denote the Gaussian probability density function with mean  $\mu$  and variance  $\sigma^2$ , and let  $\Phi(z)$  denote the standard normal cumulative distribution function. Then, for  $a \in \mathbb{R}$ ,*

$$\int \Phi(z - a) f(z|\mu, \sigma^2) dz = \Phi\left(\frac{\mu - a}{\sqrt{1 + \sigma^2}}\right).$$

Considering the probit model, we have for the  $j$ th category,  $j = 1, \dots, C$ ,  $\pi_{*j} = \Phi(\alpha_j + \mathbf{x}_*^\top \beta + u_*) - \Phi(\alpha_{j-1} + \mathbf{x}_*^\top \beta + u_*)$ , with the convention  $\alpha_0 = -\infty$  and  $\alpha_C = \infty$ , and  $\hat{f}(u_*|\mathbf{y})$  corresponds to the Gaussian density with mean  $\mu_* = \mathbb{E}[u_*|\mathbf{y}]$  given by (10), and variance  $\sigma_*^2 = \text{Var}[u_*|\mathbf{y}]$  given

by (11). Then, by (12),

$$\begin{aligned}\Pr(y_* = j|\mathbf{y}) &\approx \int \pi_{*j} \hat{f}(u_*|\mathbf{y}) \, du_* \\ &= \int \Phi(\alpha_j + \mathbf{x}_*^\top \beta + u_*) \hat{f}(u_*|\mathbf{y}) \, du_* - \int \Phi(\alpha_{j-1} + \mathbf{x}_*^\top \beta + u_*) \hat{f}(u_*|\mathbf{y}) \, du_* \\ &= \Phi\left(\frac{\mu_* + \alpha_j + \mathbf{x}_*^\top \beta}{\sqrt{1 + \sigma_*^2}}\right) - \Phi\left(\frac{\mu_* + \alpha_{j-1} + \mathbf{x}_*^\top \beta}{\sqrt{1 + \sigma_*^2}}\right).\end{aligned}$$

## Acknowledgments

Arron Gosnell was supported by a scholarship from the EPSRC Centre for Doctoral Training in Statistical Applied Mathematics at Bath (SAMBA), under the project EP/L015684/1. Arron Gosnell acknowledges Syngenta for partial funding.

## Data availability statement

The solvents data can be obtained from DOI:10.17632/b4dmjzk8w6.1.

## References

- [1] A. Agresti, *Analysis of ordinal categorical data*, Vol. 656, John Wiley & Sons, 2010.
- [2] J. Bajorath, *Chemoinformatics and Computational Chemical Biology*, Vol. 672, Humana Press, 2011.
- [3] D. Bajusz, A. Rácz, and K. Héberger, *Why is Tanimoto index an appropriate choice for fingerprint-based similarity calculations?*, J. Cheminf. 7 (2015), p. 20.
- [4] D. Baptista, J. Correia, B. Pereira, and M. Rocha, *Evaluating molecular representations in machine learning models for drug response prediction and interpretability*, J. Integr. Bioinform. 19 (2022), p. 20220006.
- [5] A. Bender and R.C. Glen, *Molecular similarity: a key technique in molecular informatics*, Org. Biomol. Chem. 2 (2004), p. 3204.
- [6] D. Bonchev, *Chemical graph theory: introduction and fundamentals*, Vol. 1, Taylor & Francis, 1991.
- [7] J.G. Booth and J.P. Hobert, *Standard errors of prediction in generalized linear mixed models*, J. Am. Stat. Assoc. 93 (1998), pp. 262–272.
- [8] L. Bornn, G. Shaddick, and J.V. Zidek, *Modeling nonstationary processes through dimension expansion*, J. Am. Stat. Assoc. 107 (2012), pp. 281–289.
- [9] M. Bouchard, A.L. Jusselme, and P.E. Doré, *A proof for the positive definiteness of the Jaccard index matrix*, Int. J. Approx. Reason 54 (2013), pp. 615–626.
- [10] S. Bouktif, A. Fiaz, A. Ouni, and M.A. Serhani, *Optimal deep learning lstm model for electric load forecasting using feature selection and genetic algorithm: Comparison with machine learning approaches*, Energies 11 (2018), p. 1636.
- [11] S.L. Chau, K. Muandet, and D. Sejdinovic, *Explaining the uncertain: Stochastic Shapley values for Gaussian process models*, Adv. Neur. In. 36 (2024).

- [12] S.S. Choi, S.H. Cha, and C.C. Tappert, *A survey of binary similarity and distance measures*, Int. J. Syst. Cybern. Inform. 8 (2010), pp. 43–48.
- [13] G. Christakos and V. Papanicolaou, *Norm-dependent covariance permissibility of weakly homogeneous spatial random fields and its consequences in spatial statistics*, Stoch. Env. Res. Risk A. 14 (2000), pp. 471–478.
- [14] W. Chu, Z. Ghahramani, and C.K.I. Williams, *Gaussian processes for ordinal regression*, J. Mach. Learn. Res. 6 (2005), pp. 1019–1041.
- [15] C. Czado and T.J. Santner, *The effect of link misspecification on binary regression inference*, J. Stat. Plan. Inference 33 (1992), pp. 213–231.
- [16] Danishuddin and A.U. Khan, *Descriptors and their selection methods in QSAR analysis: paradigm for drug design*, Drug Discov. Today 21 (2016), pp. 1291–1302.
- [17] S. Elhay and J. Kautsky, *Algorithm 655: Iqpack: Fortran subroutines for the weights of interpolatory quadratures*, ACM Trans. Math. 13 (1987), pp. 399–415.
- [18] EU Commission, *Ordinance on facilities for handling substances that are hazardous to water [German designation: AwSV]*, Notification Number: 2015/394/D (2015).
- [19] E. Evangelou and Z. Zhu, *Optimal predictive design augmentation for spatial generalised linear mixed models*, J. Stat. Plan. Inference 142 (2012), pp. 3242–3253.
- [20] P. Fenner and E. Pyzer-Knapp, *Privacy-preserving Gaussian process regression—a modular approach to the application of homomorphic encryption*, Proc. Innov. Appl. Artif. 34 (2020), pp. 3866–3873.
- [21] J.C. Gower and P. Legendre, *Metric and Euclidean properties of dissimilarity coefficients*, J. Classification 3 (1986), pp. 5–48.
- [22] J.C. Gower, *A general coefficient of similarity and some of its properties*, Biometrics (1971), pp. 857–871.
- [23] J.C. Gower and M.J. Warrens, *Similarity, Dissimilarity, and Distance, Measures of*, Wiley, 2017 5.
- [24] J.C. Gower, *Properties of Euclidean and non-Euclidean distance matrices*, Linear Algebra Appl. 67 (1985), pp. 81–97.
- [25] D.K. Hildebrand, J.D. Laing, and H. Rosenthal, *Analysis of ordinal data*, 8, Sage, 1977.
- [26] I. Kapetanovic, *Computer-aided drug discovery and development (cadd): In silico-chemico-biological approach*, Chem.-Biol. Interact. 171 (2008), pp. 165–176.
- [27] S. Katoch, S.S. Chauhan, and V. Kumar, *A review on genetic algorithm: past, present, and future*, Multimed. Tools Appl. 80 (2021), pp. 8091–8126.
- [28] S. Langner, J.A. Hauch, and C.J. Brabec, *List of organic solvents with information about Hansen solubility parameter, solvent-properties, hazardousness and cost-analysis*, Mendeley Data (2022). V1.
- [29] A.R. Leach and V.J. Gillet, *An Introduction To Chemoinformatics*, Springer Netherlands, 2007.
- [30] A. Liaw and M. Wiener, *Classification and regression by randomforest*, R News 2 (2002), pp. 18–22. Available at <https://CRAN.R-project.org/doc/Rnews/>.
- [31] A.H. Lipkus, *A proof of the triangle inequality for the Tanimoto distance*, J. Math. Chem. 26 (1999), pp. 263–265.
- [32] Y.C. Lo, S.E. Rensi, W. Torng, and R.B. Altman, *Machine learning in chemoinformatics and drug discovery*, Drug Discov. Today 23 (2018), pp. 1538–1546.

- [33] K.V. Mardia, J.T. Kent, and J.M. Bibby, *Multivariate Analysis*, Academic Press Ltd, London NA1 7DX, 1979.
- [34] P. McCullagh, *Regression models for ordinal data*, J. R. Stat. Soc., B: Stat. 42 (1980), pp. 109–127.
- [35] H.B. Moss and R.R. Griffiths, *Gaussian process molecule property prediction with FlowMO*, arXiv preprint arXiv:2010.01118 (2020).
- [36] C.R. Munteanu, E. Fernandez-Blanco, J.A. Seoane, P. Izquierdo-Novo, J.A. Rodriguez-Fernandez, J.M. Prieto-Gonzalez, J.R. Rabunal, and A. Pazos, *Drug discovery and design for complex diseases through QSAR computational methods*, Curr. Pharm. Des. 16 (2010), pp. 2640–2655.
- [37] R. Natarajan, C.E. McCulloch, and N.M. Kiefer, *A Monte Carlo EM method for estimating multinomial probit models*, Comput. Statist. Data Anal. 34 (2000), pp. 33–50.
- [38] B.J. Neves, R.C. Braga, C.C. Melo-Filho, J.T. Moreira-Filho, E.N. Muratov, and C.H. Andrade, *QSAR-based virtual screening: Advances and applications in drug discovery*, Front. Pharmacol. 9 (2018), p. 1275.
- [39] A. Paul, D. Jha, R. Al-Bahrani, W.k. Liao, A. Choudhary, and A. Agrawal, *Chemixnet: Mixed dnn architectures for predicting chemical properties using multiple molecular representations*, arXiv preprint arXiv:1811.08283 (2018).
- [40] R Core Team, *R: A Language and Environment for Statistical Computing*, R Foundation for Statistical Computing, Vienna, Austria (2021).
- [41] C.E. Rasmussen and C.K.I. Williams, *Gaussian processes for machine learning*, MIT press, Cambridge, MA, 2006.
- [42] RDKit, *Open-source cheminformatics*, <https://www.rdkit.org> (2023).
- [43] J.L. Reymond and M. Awale, *Exploring chemical space for drug discovery using the chemical universe database*, ACS Chem. Neurosci. 3 (2012), pp. 649–657.
- [44] P.J. Ribeiro Jr, P. Diggle, O. Christensen, M. Schlather, R. Bivand, and B. Ripley, *geoR: Analysis of Geostatistical Data* (2024). Available at <https://CRAN.R-project.org/package=geoR>, R package version 1.9-4.
- [45] J.A. Royle and D. Nychka, *An algorithm for the construction of spatial coverage designs with implementation in splus*, Comput. Geosci. 24 (1998), pp. 479–488.
- [46] H. Safizadeh, S.W. Simpkins, J. Nelson, S.C. Li, J.S. Piotrowski, M. Yoshimura, Y. Yashiroda, H. Hirano, H. Osada, M. Yoshida, *et al.*, *Improving measures of chemical structural similarity using machine learning on chemical-genetic interactions*, J. Chem. Inf. Model. 61 (2021), pp. 4156–4172.
- [47] P.D. Sampson and P. Guttorp, *Nonparametric estimation of nonstationary spatial covariance structure*, J. Am. Stat. Assoc. 87 (1992), pp. 108–119.
- [48] F. Sandfort, F. Strieth-Kalthoff, M. Kühnemund, C. Beecks, and F. Glorius, *A structure-based platform for predicting chemical reactivity*, Chem 6 (2020), pp. 1379–1390.
- [49] Z. Shun and P. McCullagh, *Laplace approximation of high dimensional integrals*, J. R. Stat. Soc. Ser. B. Stat. Methodol. 57 (1995), pp. 749–760.
- [50] M.C. South, G.B. Wetherill, and M.T. Tham, *Hitch-hiker’s guide to genetic algorithms*, J. Appl. Stat. 20 (1993), pp. 153–175.
- [51] V. Srivastava, C. Selvaraj, and S.K. Singh, *Chemoinformatics and QSAR*, Springer Singapore, 2021.

- [52] S.J. Swamidass, J. Chen, J. Bruand, P. Phung, L. Ralaivola, and P. Baldi, *Kernels for small molecules and the prediction of mutagenicity, toxicity and anti-cancer activity*, *Bioinform.* 21 (2005), pp. i359–i368.
- [53] R. Todeschini, V. Consonni, H. Xiang, J. Holliday, M. Buscema, and P. Willett, *Similarity coefficients for binary chemoinformatics data: overview and extended comparison using simulated and real data sets*, *J. Chem. Inf. Model.* 52 (2012), pp. 2884–2901.
- [54] J. Townsend, C.P. Micucci, J.H. Hymel, V. Maroulas, and K.D. Vogiatzis, *Representation of molecular structures with persistent homology for machine learning applications in chemistry*, *Nat. Commun.* 11 (2020), p. 3230.
- [55] N. Wen, G. Liu, J. Zhang, R. Zhang, Y. Fu, and X. Han, *A fingerprints based molecular property prediction method using the BERT model*, *J. Cheminformatics* 14 (2022), pp. 1–13.
- [56] P. Willett, *Similarity-based virtual screening using 2d fingerprints*, *Drug Discov. Today* 11 (2006), pp. 1046–1053.